Extracellular matrix protein tenascin-C is required in the bone marrow microenvironment primed for hematopoietic regeneration

Ayako Nakamura-Ishizu,[1] Yuji Okuno,[2] Yoshiki Omatsu,[3,4] Keisuke Okabe,[2,5] Junko Morimoto,[6] Toshimitsu Uede,[6] Takashi Nagasawa,[3,4] *Toshio Suda,[1] and *Yoshiaki Kubota[2]

[1]Department of Cell Differentiation, The Sakaguchi Laboratory, and [2]Center for Integrated Medical Research, School of Medicine, Keio University, Tokyo, Japan; [3]Department of Immunobiology and Hematology, Institute for Frontier Medical Sciences, Kyoto University, Kyoto, Japan; [4]Japan Science and Technology Agency, Core Research for Evolutional Science and Technology, Tokyo, Japan; [5]Department of Plastic and Reconstructive Surgery, Keio University, Tokyo, Japan; and [6]Division of Molecular Immunology, Institute for Genetic Medicine, Hokkaido University, Sapporo, Japan

The BM microenvironment is required for the maintenance, proliferation, and mobilization of hematopoietic stem and progenitor cells (HSPCs), both during steady-state conditions and hematopoietic recovery after myeloablation. The ECM meshwork has long been recognized as a major anatomical component of the BM microenvironment; however, the molecular signatures and functions of the ECM to support HSPCs are poorly understood. Of the many ECM proteins, the expression of tenascin-C (TN-C) was found to be dramatically up-regulated during hematopoietic recovery after myeloablation. The TN-C gene was predominantly expressed in stromal cells and endothelial cells, known as BM niche cells, supporting the function of HSPCs. Mice lacking TN-C (*TN-C*$^{-/-}$) mice showed normal steady-state hematopoiesis; however, they failed to reconstitute hematopoiesis after BM ablation and showed high lethality. The capacity to support transplanted wild-type hematopoietic cells to regenerate hematopoiesis was reduced in *TN-C*$^{-/-}$ recipient mice. In vitro culture on a TN-C substratum promoted the proliferation of HSPCs in an integrin α9–dependent manner and up-regulated the expression of the cyclins (*cyclinD1* and *cyclinE1*) and down-regulated the expression of the cyclin-dependent kinase inhibitors (*p57*^{Kip2}, *p21*^{Cip1}, *p16*^{Ink4a}). These results identify TN-C as a critical component of the BM microenvironment that is required for hematopoietic regeneration. (*Blood*. 2012;119(23):5429-5437)

Introduction

The BM is the main hematopoietic organ in the adult. It provides an efficient microenvironment for hematopoiesis, which contributes to the maintenance, proliferation, and differentiation of hematopoietic stem and progenitor cells (HSPCs). A well-accepted concept regarding the hematopoietic microenvironment is that of the hematopoietic stem cell (HSC) niche.[1-3] The HSC niche is subdivided into the osteoblastic niche[4-7] and the vascular niche.[8,9] The BM vasculature is surrounded by perivascular niche cells such as macrophages[10,11] and stromal cells (ie, reticular cells) of mesenchymal lineage,[12,13] which cooperatively regulate HSC activity.

In contrast to the well-investigated cellular niches, the functions of ECM proteins as a niche are poorly understood. The ECM of the BM comprises fibrous proteins such as types I and IV collagen and fibronectin (FN)[14] and nonfibrous proteins such as tenascin-C (TN-C).[15] We have shown previously that long-term bromodeoxyuridine (BrdU)–label-retaining cells reside in the hypoxic areas distant from the endothelial tubes closely attached to nonendothelial ECM structures.[16] In vitro culture systems also suggest the importance of the ECM in the maintenance of HSPCs.[17] Therefore, a role for the ECM as a BM niche has been suggested, yet little is known about how the ECM affects HSPCs in vivo.

TN-C is a highly conserved ECM glycoprotein that is expressed mainly during embryogenesis.[18] TN-C–deficient mice show normal development with no defects in gross organization.[18] In adult tissues, TN-C expression is restricted to sites of active tissue remodeling (eg, inflammation[19,20] and wound healing[21]) and plays a significant function in these pathologies.[19-21] Expression of TN-C in the BM is limited to the endosteal regions.[15,22] TN-C acts by binding with high affinity to specific integrins such as integrin α9 or to other matrix proteins such as FN.[23] The colony-forming capacity of BM cells is lower in TN-C–deficient mice, although their mononuclear cell count and BM architecture show no detectable abnormalities, suggesting a significant function of TN-C in stressed conditions.[24] The neutralizing integrin α9 inhibits HSPC proliferation and adhesion to primary cultured osteoblasts.[25] TN-C displays cytoadhesive properties toward hematopoietic cells in in vitro adhesion assays[15]; however, the role played by TN-C during hematopoiesis in vivo is still unclear.

In the present study, we identified a prominent role for TN-C in BM reconstitution after myeloablation. TN-C expression in the BM was highly up-regulated, becoming much more widely distributed after 5-fluoruracil (5-FU) administration. TN-C–deficient mice (*TN-C*$^{-/-}$) showed impaired BM recovery and high lethality after myeloablation. In addition, TN-C promoted the proliferation of HSPCs both in vivo and in vitro. The results of the present study demonstrate a requirement for TN-C in the BM microenvironment primed for hematopoietic regeneration.

Submitted November 19, 2011; accepted April 25, 2012. Prepublished online as *Blood* First Edition paper, May 2, 2012; DOI 10.1182/blood-2011-11-393645.

*T.S. and Y.K. contributed equally to this work.

The online version of this article contains a data supplement.

The publication costs of this article were defrayed in part by page charge payment. Therefore, and solely to indicate this fact, this article is hereby marked "advertisement" in accordance with 18 USC section 1734.

Methods

Mice

All mice were of a C57BL/6 background. *TN-C*–deficient mice were obtained from the RIKEN BioResource Center.[26] All animal experiments were approved by Keio University and performed in accordance with the guidelines of Keio University for animal and recombinant DNA experiments.

5-FU administration and sublethal irradiation

Myeloablation was induced by either 5-FU (Sigma-Aldrich) as an IP injection at 250 mg/kg body weight or sublethal irradiation (6.5 Gy). Peripheral blood counts were measured at 3-day intervals. Briefly, peripheral blood was collected from the tail vein in a heparinized microtube (Drummond Scientific) and analyzed using CellTac (Nihon Kohden). Mice were killed at the indicated times after 5-FU administration.

Abs

The primary Abs used for immunohistochemistry (IHC) were hamster anti-CD31 Ab (2H8; Millipore), rat anti–CD31 Ab (MEC13.3; BD Biosciences), and anti–TN-C Ab (Abcam). The primary polyclonal Abs were FN (DAKO), collagen IV (Cosmo Bio), laminin (Sigma-Aldrich), and c-Kit (R&D Systems). Secondary Abs were Alexa Fluor 488–conjugated IgGs (Molecular Probes) or Cy3/Cy5/DyLight549/DyLight649–conjugated IgGs (Jackson ImmunoResearch). Specimens were treated with DAPI (Molecular Probes) for nuclear staining. For blocking the function of integrin α9 in vitro, hamster mAbs against murine integrin α9 (clone 55A2C)[27] were used. As a negative control study, we used anti-integrin α9 Abs (clone 18R18D)[27] that do not have such an inhibitory effect.

Immunostaining of BM

Isolated femurs were fixed in 4% paraformaldehyde in PBS overnight at 4°C and then immersed in 0.5M EDTA solution for at least 7 days for decalcification. Femurs were embedded in optimal cutting temperature compound (Tissue Tek) and cryosections (12 μm) were made. For IHC, samples were stained with primary Abs overnight at 4°C. Staining with secondary Abs was done for 1 hour at room temperature. Thereafter, samples were postfixed in 4% paraformaldehyde and mounted using a Prolong Antifade Kit (Molecular Probes). For the BrdU incorporation assay, 100 μg of BrdU (BD Pharmingen) per gram of body weight was dissolved in sterile PBS and injected intraperitoneally 2 hours before animals were killed. Prepared sections were stained using a BrdU IHC system (Calbiochem).

Confocal microscopy

Fluorescent images were obtained using a confocal laser scanning microscope (FV1000-D; Olympus) at room temperature. Scanning was performed in sequential laser emission mode to avoid scanning at other wavelengths. The images in Figures 1 through G, 2C through E, 4A, and B, H through K, 6A through E and supplemental Figure 1D through L were digitally recorded with a high magnification objective lens (40×/1.3 NA oil objective) to minimize their pseudo-positive detection of the neighboring layers, while the other images (Figure 1A-F) were scanned with a low magnification lens (10×/0.4 NA). FV10-ASW Viewer 3.0 software (Olympus) was used to process the images (brightness and contrast), and export them as .jpg format. For image acquisition of samples stained with H&E (supplemental Figure 1A-C), an inverted microscope (CKX41; Olympus) equipped with an objective lens (10×/0.4 NA) and a digital camera (DP20; Olympus) was used at room temperature. For constructing merged images for quadruple immunohistochemistry (Figure 1I), triple colored images were overlaid with DAPI using Adobe Photoshop CS2 and were exported as .jpg format. Quantification of substances of interest was performed in fields of view per sample in each scanned image with a high magnification objective lens (40×/1.3).

Quantitative PCR assay

Total RNA was prepared from BM at the indicated times after 5-FU administration and reverse transcribed using Superscript II (Invitrogen). Quantitative PCR assays were performed using an ABI 7500 Fast Real-Time PCR System, TaqMan Fast Universal PCR Master Mix (Applied Biosystems), and a TaqMan Gene Expression Assay Mix comprising *cyclinD1* (Mm03053889_s1), *cyclinD2* (Mm00438070_m1), *cyclinD3* (Mm01612362_m1), *cyclinE1* (Mm01266311_m1), *cyclinE2* (Mm00432367_m1), *cyclinG1* (Mm00438084_m1), *cyclinG2* (Mm01354285_m1), $p21^{Cip1}$ (Mm00432448_m1), $p57^{Kip2}$ (Mm01272135_g1), $p16^{Ink4a}$ (Mm00494449_m1), $p18^{Ink4c}$ (Mm00483243_m1), *fn1* (Mm01256744_m1), *itgna4* (Mm00439770_m1), *itgna5* (Mm00439797_m1), *itgna7* (Mm00434400_m1), *itgna9* (Mm00519293_m1), *itgnav* (Mm00434506_m1), *itgnb1* (Mm01253227_m1), *itgnb3* (Mm00443980_m1), *itgnb6* (Mm01269869_m1), c-*myc* (Mm00487803_m1), and *tn-c* (Mm00495662_m1). A mouse β-*actin* (Mm00607939_sl) assay mix served as an endogenous control. Data were analyzed using 7500 Fast System SDS Version 1.3.1 software. Each experiment was performed with 4 replicates from each sample and the results were averaged.

Flow cytometry

Dissected tibias and femurs were flushed with 2% FCS in PBS using a 23-gauge needle. The dissociated BM cells were collected and BM mononuclear cells (BMMNCs) isolated by density centrifugation on Lymphoprep (Axis-Shield). BMMNCs were preincubated with Fc block (BD Biosciences) to avoid nonspecific binding of Abs, and then incubated with the intended Abs. The primary Abs (BD Biosciences) used were: anti–c-Kit (2B8), anti–Sca-1 (E13-161.7), anti-CD4 (L3T4), anti-CD8 (53-6.72), anti-B220 (RA3-6B2), anti–TER-119, anti–Gr-1 (RB6-8C5), anti-CD11b (M1/70), anti-CD3 (500A2), anti-Flt3 (AF10.1), anti-CD31 (MEC13.3), anti-CD41 (MWRReg30), anti-CD45.2 (104), and anti-CD45.1 (A20). Primary Abs from other manufactures included anti-integrin α9 (AF3827; R&D Systems), anti-integrin β1 (Ha2/5; BD Biosciences), anti-CD34 (KAM34; eBiosciences), anti-PDGFRα (APA5; eBiosciences), anti-CD48 (B120132; BioLegend), and anti-CD150 (TC15-12F12.2; BioLegend). A mixture of CD4, CD8, B220, TER-119, Mac-1, and Gr-1 was used as the lineage (Lin) mixture. Propidium iodide was used to identify and exclude dead cells. Stained cells were analyzed and sorted using a SORP FACSAria (BD Biosciences) and the data analyzed with FlowJo 7.6.3 software (TreeStar). For cell-cycle analyses of HSCs, BrdU (1 mg) was injected intraperitoneally 4 times at 12-hour intervals before the animals were killed. HSC fractions were sorted, fixed on MAS-coated slides (Matsunami) and stained using a BrdU IHC system (Calbiochem).

BM transplantation (BMT)

BMMNCs were obtained from *TN-C*$^{+/+}$, *TN-C*$^{-/-}$, or Ly5.1 mice as described in "Flow cytometry." *TN-C*$^{+/+}$ or *TN-C*$^{-/-}$ mice-derived BMMNCs (2×10^5 cells or 1×10^4 cells) were transplanted into lethally irradiated Ly5.1 mice. For reverse BMT, BMMNCs from C57Bl/6-Ly5.1 mice (2×10^5) were transplanted into lethally irradiated *TN-C*$^{+/+}$ or *TN-C*$^{-/-}$ mice (Ly5.2). Peripheral blood chimerisms in recipient mice were analyzed at 1-month intervals. Recipient mice were killed for analyses 4 months after BMT.

LSK cell culture on TN-C substrata

Recombinant full-length human TN-C (R&D Systems) or recombinant proteins of a FN type III repeat domain of human TN-C lacking the arginine-glycine-aspartic acid (RGD) sequence (TN-C^{FNIII})[27]at a concentration of 2 μg/cm^2 was coated onto FN-coated culture slides (BD Biosciences) for 1 hour at 37°C. FACS-sorted $Lin^-Sca1^+c\text{-}Kit^+$ (LSK) cells were obtained and cultured on FN with or without TN-C/TN-C^{FNIII} in SF-O3 medium (Sanko Junyaku) containing 100 ng/mL of SCF and 100 ng/mL of thrombopoietin for 48 hours. Before staining, cultured cells were incubated with BrdU (3 μg/mL of medium) for 2 hours and then fixed with methanol and stained using a BrdU IHC system (Calbiochem). For neutralizing α9 integrin, the culture medium was supplemented with hamster mAbs against murine integrin α9 (55A2C or 18R18D) at a concentration of 10μg/mL, as described previously.[27]

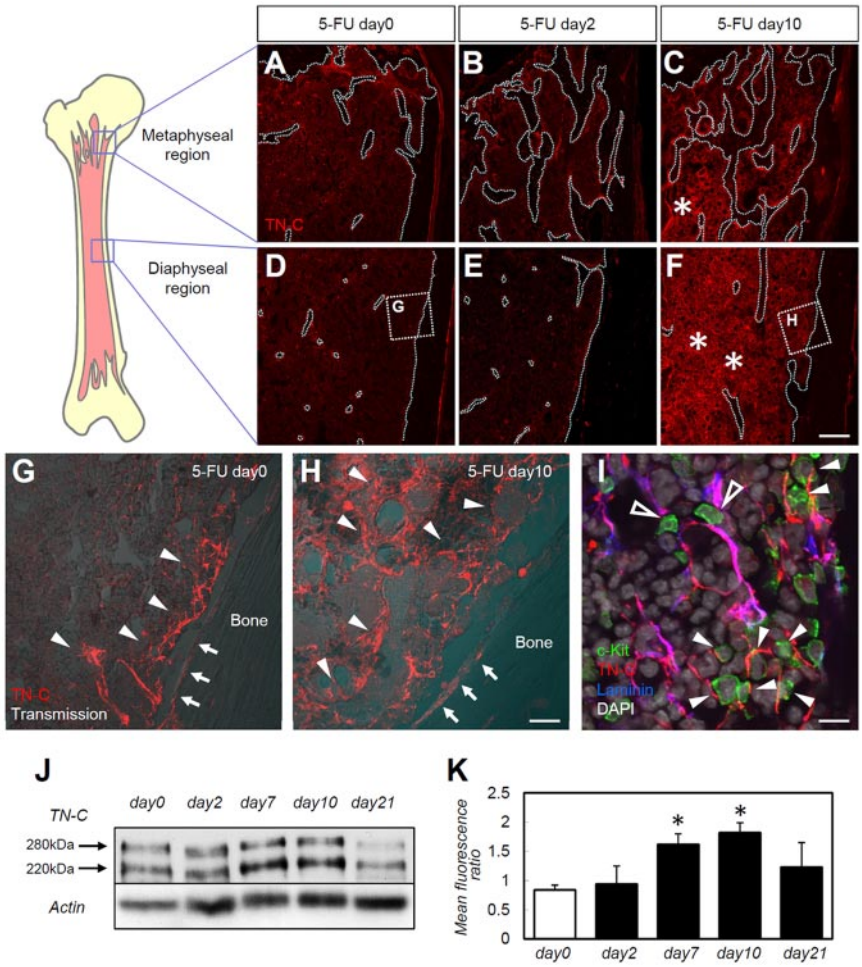

Figure 1. TN-C is markedly up-regulated in the BM during myeloablation and hematopoietic recovery. BM sections from days 0, 2, and 10 stained for TN-C (red) in the metaphyseal (A-C) and diaphyseal (D-F) regions of the femoral bone. The bone surfaces are outlined by white dotted lines (A-F). The asterisks in panels C and F show the up-regulation of TN-C beyond the endosteal areas in both the metaphyseal and diaphyseal regions. (G-H) Enlargement of the dotted squares in panels D and F. Arrows indicate the bone surface; arrowheads indicate stromal TN-C expression. (I) High magnification of day 10 BM samples stained for TN-C (red), c-Kit (green), laminin (blue), and DAPI (gray). c-Kit$^+$ cells adhered to TN-C expressed perivascularly (costained with laminin; open arrowheads) or away from the vasculature (arrowheads). (J) Western blotting for TN-C in total BM proteins showed that TN-C proteins were detected in 2 bands at 280 and 220 kDa. (K) Quantification of Western blot expression. The mean fluorescence ratio was calculated by dividing the mean fluorescence of the TN-C band by that of the corresponding β-actin band. *$P < .05$. Scale bars indicate 200 μm in panels A through F; 40 μm in panels G and H; and 10 μm in panel I.

Western blotting

Western blot analysis was performed as described previously[28] using anti–TN-C (Abcam) as the primary Ab. The amount of total protein was examined by reblotting with anti–β-actin (Sigma-Aldrich).

Statistical analysis

All results are expressed as the means ± SD. The 2-tailed Student *t* test and the log-rank test were used for comparisons between 2-group experiments. The Wilcoxon signed-rank test was performed on complete blood counts after 5-FU administration.

Results

TN-C is up-regulated and widely distributed in the BM during hematopoietic recovery after myeloablation

First, we examined the BM expression of various ECM proteins during steady-state hematopoiesis, immediately after myeloablation, and during hematopoietic recovery. As described previously,[5] injection of 5-FU resulted in a marked reduction of BM cellularity on day 2 after 5-FU administration, and recovery was evident by day 10 (supplemental Figure 1A-C, available on the *Blood* Web site; see the Supplemental Materials link at the top of the online article). A reduction in (day 2) and recovery of (day 10) BM c-Kit$^+$ HSPC numbers was also noted (data not shown). Only a moderate distortion of ECM components (ie, FN, laminin, and type IV collagen) was noted at day 10 (supplemental Figure 1D-L). TN-C expression showed a far more drastic change during hematopoietic recovery compared with that of the other ECM molecules. Before 5-FU administration, and as described previously,[17] TN-C expression was limited to the periosteal regions (Figure 1A,D,G), with abundant expression in the trabecular bone–rich metaphyseal regions compared with the diaphyseal regions. TN-C protein was detected both on the bone surface (Figure 1G arrows) and in the stromal regions near the bone (Figure 1G arrowheads). TN-C expression did not change on day 2 (Figure 1B,E), but was markedly up-regulated on day 10 after 5-FU administration. TN-C expression increased and the protein was widely distributed throughout both the metaphyseal (Figure 1C) and diaphyseal (Figure 1F,H) regions. TN-C proteins were detected in the central stromal (Figure 1H arrowheads) and endosteal regions (Figure 1H arrows). HSPCs labeled by c-Kit Abs were observed in close contact with TN-C proteins (Figure 1I). Laminin was stained to highlight the endothelial cell basement membrane (supplemental Figure 1G-I) to discriminate perivascular TN-C from TN-C expressed further from the vasculature (Figure 1I). HSPCs resided in close contact with TN-C expressed in both locations, suggesting a functional association between HSPCs and TN-C rather than simply reflecting the well-known association between HSPCs and endothelial cells.[8,9] The increase in TN-C expression after 5-FU administration was confirmed by Western blotting (Figure 1J-K). TN-C expressions returned to steady-state levels by day 21 (Figure 1J-K).

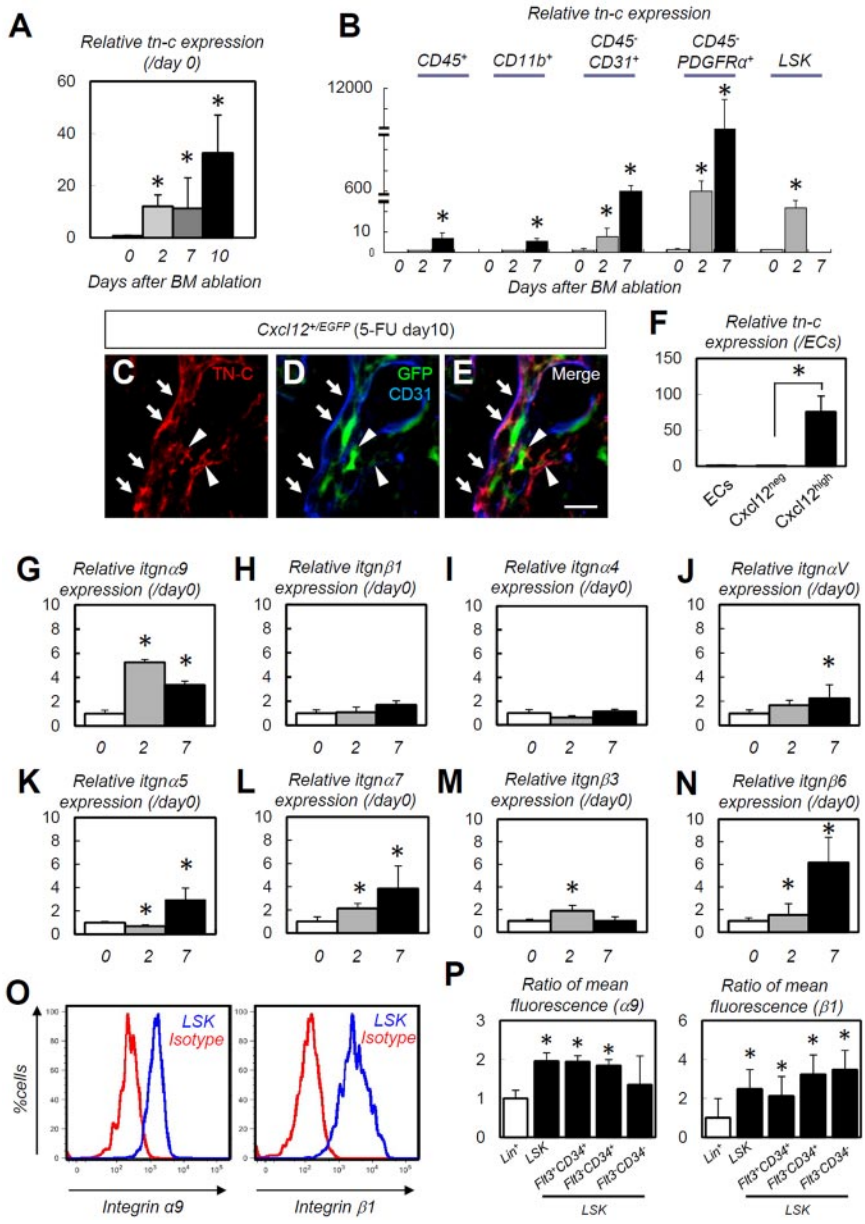

Figure 2. TN-C is predominantly expressed in stromal and endothelial cells and its ligand, integrin α9, is expressed on HSPCs. (A-B) Relative RT-PCR for TN-C mRNA expression on whole-BM (A) and on $CD45^+$, $CD11b^+$, $CD31^+CD45^-$, $PDGFR\alpha^+CD45^-$, and LSK cells (B; n = 5). (C-E) IHC of BM obtained from *Cxcl12*$^{+/EGFP}$ mice on day 10. Note that TN-C proteins (red) are deposited around $CD31^+$ (blue) endothelial cells (arrows) or CAR cells (green; arrowheads). (F) Relative expression of TN-C mRNA in isolated $CD45^-Ter119^-CD31^+Sca1^+$ (ECs), $Cxcl12^{neg}$ and $Cxcl12^{high}$ cells on day 10 (n = 5). (G-N) Relative expressions of integrin α9 (G), integrin β1 (H), integrin α4 (I), integrin αV (J), integrin α5 (K), integrin α7 (L), integrin β3 (M), and integrin β6 (N) in whole BM cells (n = 6). (O) Flow cytometric analysis of integrin α9 and integrin β1 expression by LSK cells. (P) Ratio (Lin^+ = 1) of mean fluorescence for integrin α9 and integrin β1 in the Lin^+ and LSK fractions (n = 7). *$P < .05$. Scale bar indicates 50 μm.

TN-C is predominantly expressed in stromal and endothelial cells and its ligand, integrin α9, is expressed on HSPCs

We also performed a detailed analysis of cellular TN-C mRNA expression. TN-C mRNA expression in the entire BM was markedly up-regulated after 5-FU administration (Figure 2A). The immunofluorescence data (Figure 1I) indicated that TN-C was produced by endothelial cells, along with some other lineage cells. PDGFRα is expressed in BM stromal cells.[29] A prominent up-regulation in TN-C gene expression was noted in the $CD45^-CD31^+$ endothelial cell and $CD45^-PDGFR\alpha^+$ stromal cell populations after 5-FU administration. The $CD45^+$, $CD11b^+$ or LSK cell populations showed far lower expression than stromal and endothelial cells, although these cell populations also exhibited significant up-regulation of TN-C after 5-FU administration (Figure 2B and supplemental Figure 2). CXCL-12–abundant reticular (CAR) cells, a subpopulation of stromal cells, are required for the proliferation and maintenance of HSCs.[12,30] IHC of BM samples from *Cxcl12*$^{+/EGFP}$ knock-in mice showed that some of the CAR cells were positive for TN-C (Figure 2C-E arrowheads). TN-C mRNA was much more abundant in CAR cells than in $Cxcl12^-$ cells and endothelial cells (Figure 2F), suggesting that CAR cells are a major cellular source of TN-C.

TN-C exerts its effects by binding to multiple integrins and ECM components[31]; of these, integrin α9 binds to the FN-III domain of TN-C and promotes the proliferation of neurons.[32] Whole-BM mRNA transcript levels for *itgnα9*, *αV*, *α5*, *α7*, *b3*, and *β6* were significantly up-regulated during hematopoietic recovery (Figure 2G,J-N). In particular *itgnα9* showed prompt and explicit up-regulation as early as 2 days after 5-FU treatment, whereas *itgnαV*, *α5*, *α7*, and *β6* exhibited more gradual and moderate up-regulation. The transcription levels of other integrins, such as *itgnβ1* (Figure 2H) and *itgnα4* (Figure 2I), were not significantly up-regulated. Consistent with the findings of Nilsson et al,[33,34] flow cytometric analysis revealed that LSK cells expressed high levels

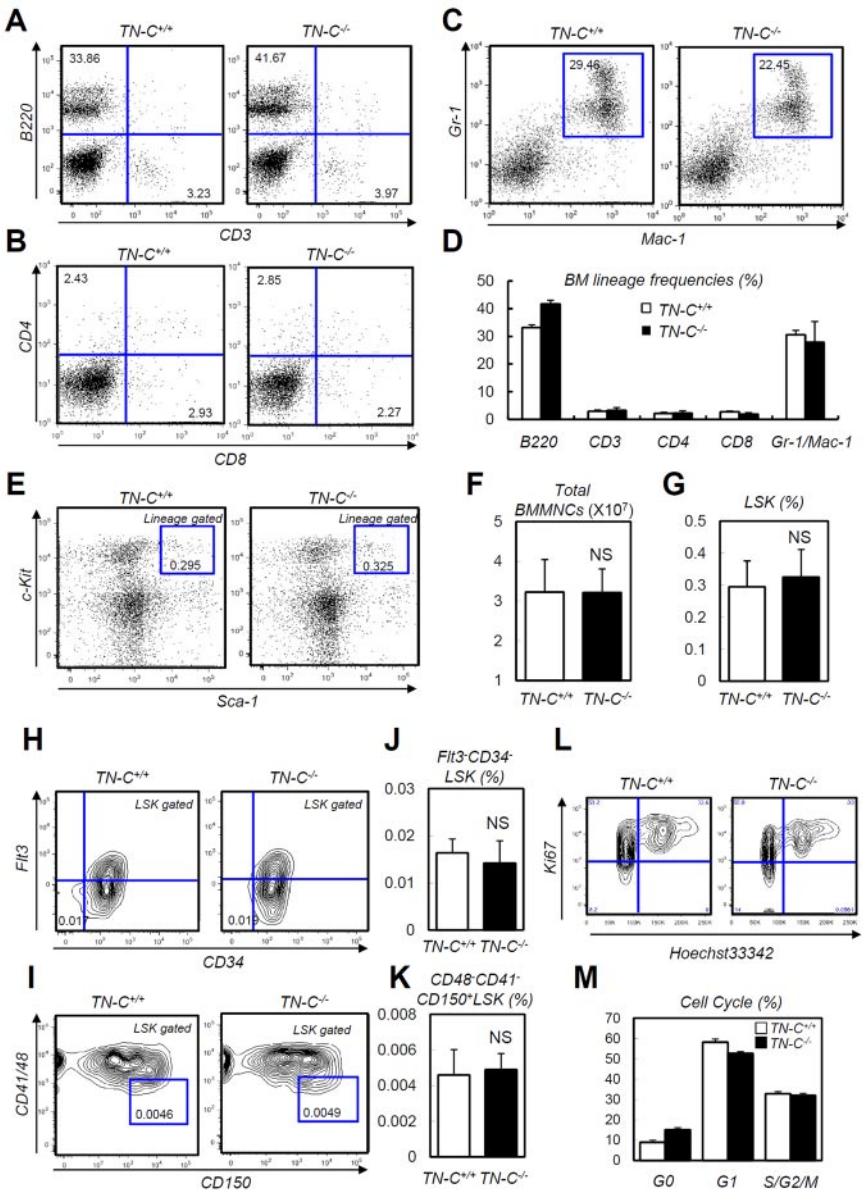

Figure 3. Normal steady-state hematopoiesis in *TN-C*$^{-/-}$ mice. (A-C) FACS plots showing BM lineage frequency. (D) Quantification in each lineage (n = 4). (E) FACS plot showing the detection of LSK cells. (F-G) Total MNC count (F) and LSK cell count (G; n = 4). (H-K) FACS plots (H-I) and quantification (n = 4; J-K) of Flt3$^-$CD34$^-$ LSK and CD48$^-$CD41$^-$CD150$^+$ LSK cell frequency. (L-M) Cell-cycle status frequencies assessed through Ki-67 and Hoechst staining of LSK cells (n = 6). *$P < .05$.

of integrin α9 (Figure 2O). Integrin β1, a binding partner of integrin α9, was also highly expressed in HSC fractions (Figure 2O). Quantification of mean fluorescence showed that integrin β1 was expressed strongly in primitive HSCs (Flt3$^-$CD34$^+$ or Flt3$^-$CD34$^-$ LSKs)[35,36] compared with the Flt3$^+$CD34$^+$ cell fraction, although integrin α9 was evenly expressed in those subpopulations (Figure 2P). These results suggest that the expression of TN-C is predominant in stromal and endothelial cells and its ligand, integrin α9β*1*, is highly expressed on HSPCs.

TN-C–deficient mice show defects in hematopoietic recovery after 5-FU treatment and sublethal irradiation

The expression analysis described in the previous section suggested that TN-C functions during BM reconstitution. Before analyzing the function of TN-C during hematopoietic recovery, we checked the steady-state status of *TN-C*$^{-/-}$ mice, which did not show apparent defects in steady-state hematopoietic parameters, including peripheral blood counts, total BM cellularity, HSC frequency, and BM lineage composition (Figure 3A-K). For assessing the proliferation rate in HSPCs, we stained LSK cells from *TN-C*$^{+/+}$ and *TN-C*$^{-/-}$ mice with Ki67 and Hoechst 33342 and found no significant difference in cell-cycle frequencies (Figure 3L-M).

We next challenged TN-C–deficient mice with 5-FU–induced myeloablation. TN-C immunoreactivity, which was detected in wild-type control (*TN-C*$^{+/+}$) mice, was not detected in *TN-C*$^{-/-}$ mice (Figure 4A-B), confirming the specificity of the TN-C Ab used. *TN-C*$^{-/-}$ mice showed a significantly high level of lethality (Figure 4C) compared with *TN-C*$^{+/+}$ mice after 5-FU administration, and peripheral blood counts showed a significant delay in the recovery of WBC, hemoglobin, and platelet counts (Figure 4D-F). No differences in BM lineage frequencies were noted during hematopoietic recovery after 5-FU administration (Figure 4G). Within the BM of the *TN-C*$^{-/-}$mice, c-Kit$^+$ HSPCs were dramatically reduced in number compared with those in *TN-C*$^{+/+}$ mice (Figure 4H-I,L). Furthermore, BrdU incorporation into

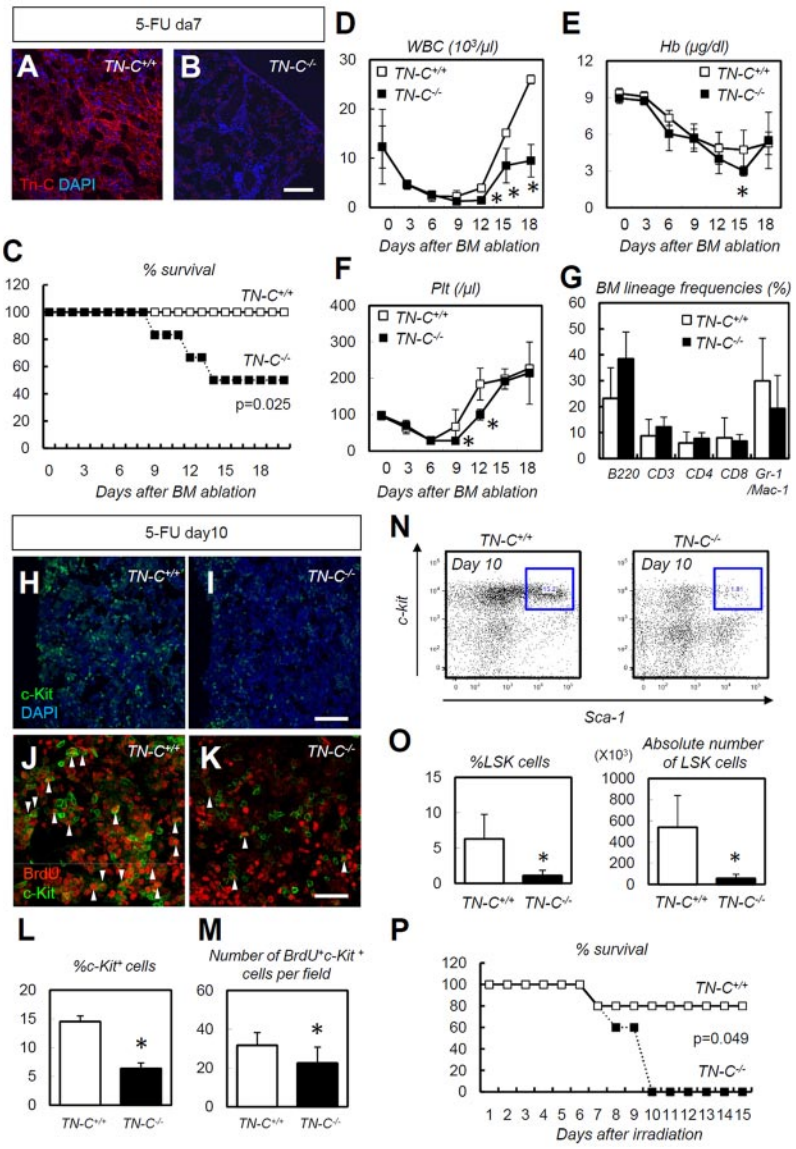

Figure 4. *TN-C*$^{-/-}$ mice show impaired hematopoietic recovery after 5-FU administration. (A-B) IHC for TN-C (red) and DAPI (blue) for day 7 BMs. *TN-C*$^{-/-}$ mice lack TN-C immunoreactivity. (C) Survival curve for *TN-C*$^{+/+}$ and *TN-C*$^{-/-}$ mice after 5-FU administration (n = 12; combination of 3 independent experiments). (D-F) Peripheral blood counts for WBCs (D), hemoglobin (Hb; E), and platelets (Plt; F) after 5-FU administration. (G) BM lineage frequencies on day 10 after 5-FU administration (n = 4). (H-I) IHC for c-Kit (green) and DAPI (blue) in *TN-C*$^{+/+}$ and *TN-C*$^{-/-}$ BM on day 10 after 5-FU administration. (J-K) IHC for BrdU (red) and c-Kit (green) in *TN-C*$^{+/+}$ and *TN-C*$^{-/-}$ BM on day 10 after 5-FU administration. (L) Quantification of the percentage of c-Kit$^+$ cells among DAPI$^+$ BM cells (n = 6). (M) Quantification of the percentage of BrdU$^+$ cells among c-Kit$^+$ cells (n = 6). (N-O) FACS plot and quantification showing the detection of LSK cells on day 10 after 5-FU administration (n = 4). (P) Survival curves for TN-C$^{+/+}$ and TN-C$^{-/-}$ mice subjected to 6.5 Gy irradiation (n = 5; combination of 3 independent experiments). *$P < .05$. Scale bars indicate 100 μm in panels A, B, H, and I and 20 μm in panels J and K.

c-Kit$^+$ HSPCs was significantly lower in the *TN-C*$^{-/-}$ BM (Figure 4J-K,M). Flow cytometry revealed a significantly lower LSK cell frequency in *TN-C*$^{-/-}$ mice on day 10 after 5-FU administration (Figure 4N-O). Similarly, increased lethality and impairment of hematopoietic recovery was observed in *TN-C*$^{-/-}$ mice when myeloablation was induced by sublethal irradiation (6.5 Gy; Figure 4P).

TN-C$^{-/-}$ mice are vulnerable recipients to BMT

Regarding the susceptibility to 5-FU and irradiation of *TN-C*$^{-/-}$ mice (Figure 4), the expression pattern of TN-C (Figure 2) indicated that it is particularly important in the nonhematopoietic BM stroma. To test this hypothesis, a series of BMTs were conducted. First, donor cells (2×10^5 BMMNCs) isolated from *TN-C*$^{+/+}$ or *TN-C*$^{-/-}$ mice (Ly5.2) were transplanted into lethally irradiated Ly5.1 mice (n = 10 for each group). There was no difference in the survival rates between the groups (data not shown). Examination of peripheral blood chimerism at 1-month intervals also showed no difference between the 2 groups (Figure 5A). BM cellularity, LSK cell frequency, and chimerism were also equivalent between the 2 groups 4 months after transplantation (Figure 5B-D). We next investigated whether TN-C deficiency in the recipient mice affected BM reconstitution during transplantation. BMMNCs (2×10^5 or 1×10^4 cells) from Ly5.1 mice were transplanted into lethally irradiated *TN-C*$^{-/-}$ or *TN-C*$^{+/+}$ mice (Ly5.2). When 2×10^5 BMMNCs were transplanted, the survival rates were the same for both groups (Figure 5E). Flow cytometric analysis of the BM of recipient mice at 4 months after BMT revealed normal frequency (Figure 5F) and chimerism (Figure 5G) of Flt3$^-$CD34$^-$LSK cells and CD48$^-$CD41$^-$CD150$^+$LSK cells; however, when the recipients were challenged with 1×10^4 BMMNCs, none of the *TN-C*$^{-/-}$ recipient mice survived beyond day 15 after BMT compared with 40% of *TN-C*$^{+/+}$ recipients (Figure 5E). Four months after BMT with 2×10^5 BMMNCs, recipient *TN-C*$^{+/+}$ or *TN-C*$^{-/-}$ mice were subjected to 5-FU–induced myeloablation. The *TN-C*$^{-/-}$ recipients showed higher levels of lethality (Figure 5J) and a delay in hematopoietic recovery in the peripheral blood (Figure 5K-M). This confirmed that the impairment of hematopoietic recovery in *TN-C*$^{-/-}$ mice was attributable to TN-C deficiency in the hematopoietic microenvironment rather than in the hematopoietic cells.

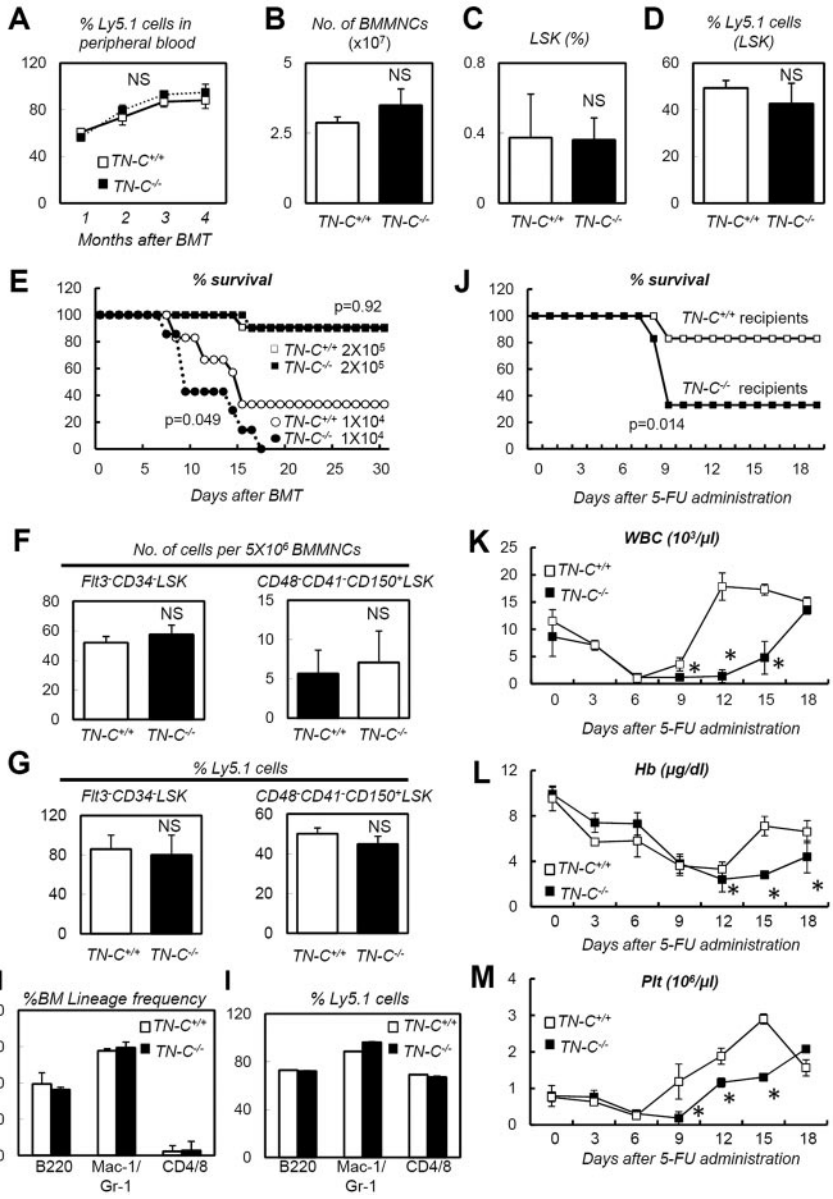

Figure 5. *TN-C*$^{-/-}$ mice are vulnerable recipients for BMT. (A) Peripheral blood chimerism analyses of recipient mice infused with 2×10^5 donor cells from *TN-C*$^{+/+}$ or *TN-C*$^{-/-}$ mice (n = 10). (B-D) BMMNC count (B), LSK cell frequency (C), and LSK cell chimerism (D) of recipient mice 4 months after transplantation with 2×10^5 donor cells from *TN-C*$^{+/+}$ and *TN-C*$^{-/-}$ mice (n = 4). (E) Survival curves for *TN-C*$^{+/+}$ and *TN-C*$^{-/-}$ recipient mice infused with 2×10^5 cells (white and black boxes, respectively) or 1×10^4 cells (white and black circles, respectively; n > 10 for each group; combination of 3 independent experiments). (F-G) Flow cytometric analysis of the BM in *TN-C*$^{+/+}$ or *TN-C*$^{-/-}$ recipient mice 4 months after BMT (2×10^5 cells) showing the frequency and chimerism of Flt3$^-$CD34$^-$ LSK cells and CD48$^-$CD41$^-$CD150$^+$ LSK cells (n = 4). (H-I) BM lineage composition (H) and chimerism (I) of cells within each lineage in the BM of *TN-C*$^{+/+}$ or *TN-C*$^{-/-}$ recipient mice 4 months after BMT (2×10^5 cells; n = 4). (J) Survival curves for *TN-C*$^{+/+}$ and *TN-C*$^{-/-}$ recipient mice challenged with 5-FU 4 months after BMT (2×10^5 cells; n = 10; combination of 3 independent experiments). (K-M) Peripheral blood counts of mice shown in panel J (n = 10). $^*P < .05$.

TN-C coating enhances in vitro proliferation and expression of cell-cycle–promoting genes in HSPCs in an integrin α9–dependent manner

The in vivo data indicated that HSPC adhesion to TN-C proteins increases HSPC proliferation. To confirm this finding, we also performed in vitro experiments using cultured HSPCs. The TN-C substratum works cooperatively with the FN substratum in vitro; the TN-C substratum alone is not effective.[37] Indeed, TN-C and FN share a common receptor, integrin α9.[38,39] Culture on slides coated with TN-C plus FN yielded significantly more BrdU$^+$ proliferating LSK cells than culture on slides coated with FN alone (Figure 6A-B,F). We also investigated whether the binding action of TN-C to integrin α9 is indeed important for the HSPC-expanding effects of TN-C. The effects of TN-C proteins was abrogated by neutralizing Abs for integrin α9 (55A2C),[27] whereas nonfunctional anti-integrin α9 Abs (18R18D)[27] did not show such inhibitory effects (Figure 6B,D,F). Furthermore, we used synthesized proteins of a FN type III repeat domain of TN-C lacking the RGD sequence (TN-C^{FNIII}),[27,40] which bind integrin α9 but not other integrins such as integrin αVβ3 and α5β1.[27,40] TN-C^{FNIII} enhanced the proliferation of LSK cells when combined with FN (Figure 6A,C,F), an effect that was abrogated by 55A2C but not 18R18D[27] (Figure 6C,E-F).

We next examined changes in cell-cycle–related genes. TN-C coating enhanced the expression of the cell-cycle–promoting genes *c-myc*, *cyclinD1*, *cyclin E1*, and *cyclinG2*, and suppressed the cell-cycle–inhibitory genes *p57*^{Kip2}, *p18*^{Ink4c}, *p21*^{Cip1}, and *p16*^{Ink4a} (Figure 6G). To determine the correlation between the in vitro and in vivo settings in regard to these cell-cycle regulators, we quantified the expression of these genes in LSK cells in *TN-C*$^{-/-}$ mice on day 10 after 5-FU administration (supplemental Figure 4). As expected, the expression of some cell-cycle–promoting genes (*cyclin D3*, *cyclin E1*, and *cyclin G2*) was down-regulated in the cells derived from *TN-C*$^{-/-}$ mice. However, some cell-cycle–inhibitory genes (*p57*^{Kip2} and *p18*^{Ink4c}) were not significantly changed and others (*p21*^{Cip1} and *p16*^{Ink4a}) were rather down-regulated in *TN-C*$^{-/-}$ mice, suggesting that down-regulated cyclins dominate the changes in cell-cycle–inhibitory genes in *TN-C*$^{-/-}$ mice.

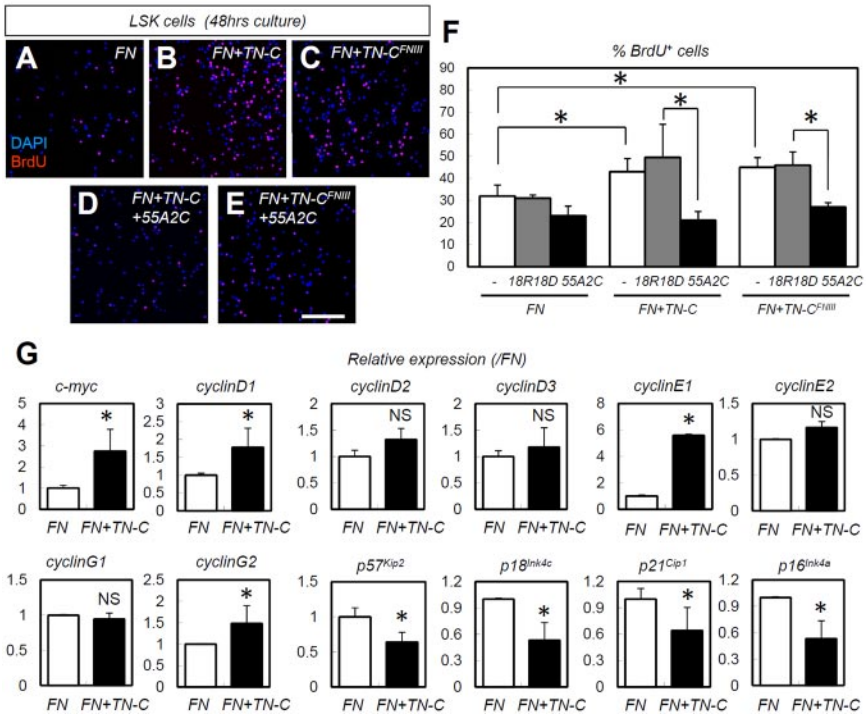

Figure 6. TN-C coating enhances the in vitro proliferation and expression of cell-cycle–promoting genes in HSPCs in an integrin α9–dependent manner. (A-E) Short-term BrdU incorporation assay for LSK cells cultured for 48 hours on slides coated with FN alone, FN plus full-length TN-C (FN + TN-C), or FN plus TN-C^{FNIII} (FN + TN-C^{FNIII}) with functional integrin α9 Abs (55A2C) or nonfunctional integrin α9 Abs (18R18D). (F) Percentage of BrdU$^+$LSK cells in panels A-E (n = 4). (G) Relative mRNA expression for the cell-cycle regulators *c-myc*, *cyclinD1*, *cyclinD2*, *cyclinD3*, *cyclinE1*, *cyclinE2*, *cyclinG1*, *cyclinG2*, *p57*^{Kip2}, *p18*^{Ink4c}, *p21*^{Cip1}, and *p16*^{Ink4a} (n = 4). *$P < .05$.

Discussion

The results of the present study show that changes in the amount and distribution of TN-C are most prominent for various ECM proteins during hematopoietic recovery after myeloablation. The TN-C gene was predominantly expressed in endothelial cells and stromal cells, including CAR cells. *TN-C*$^{-/-}$ mice were vulnerable to myeloablation because of meager levels of an HSPC-supportive environment. The results of this study identify TN-C as a critical component of the BM microenvironment that is required for hematopoietic regeneration.

TN-C$^{-/-}$ mice showed high levels of lethality and defective hematopoietic recovery after myeloablation induced by 5-FU, sublethal irradiation, or BMT using low numbers of donor cells. However, *TN-C*$^{-/-}$ recipients of BMT were rescued by higher donor cell doses. Moreover, *TN-C*$^{-/-}$ mice did not show any prominent defects in steady-state hematopoiesis, indicating that other factors may compensate for TN-C deficiency. TN-C associates with FN, and these 2 proteins work cooperatively; indeed, TN-C and FN share a common receptor, integrin α9,[38,39] neutralization of which inhibits HSPC proliferation and adhesion to primary cultured osteoblasts.[25] Because TN-C expression colocalized with FN (data not shown), it is plausible to assume that TN-C interacts functionally with FN. A significant induction of TN-C expression in response to 5-FU was also detected in hematopoietic cells (Figure 2B). Moreover, it was shown previously that the colony-forming capacity of BM cells is lower in TN-C–deficient mice.[24] These results suggest that hematopoietic cells also contribute to the deposition of TN-C proteins in the BM microenvironment and that TN-C in these cells plays a role (although not so drastic a role as in the stromal side).

In vitro culture of HSPCs on a TN-C substratum enhanced their proliferation. In addition, we showed that integrin α9, for which TN-C shows the highest affinity of all of the integrins, was expressed abundantly on LSK cells. TN-C acts as either a positive or negative regulator of cell functions such as proliferation,[41] migration,[42] and cell spreading.[37] The binding of TN-C to integrin α9 results in the phosphorylation of FAK and Erk2 in colon carcinoma cells and thereby facilitates cell proliferation.[31] The high frequency of integrin α9 on HSPCs suggests that these cells bind to TN-C and subsequently proliferate. In the present study, we found that TN-C is expressed beyond the endosteal regions during BM reconstitution. This expansion may enable HSPCs to migrate to a more spacious location for proliferation and differentiation rather than being stationed in the endosteal zone. Osteopontin, another ligand for integrin α9, is mainly expressed in the endosteal regions of the BM and thereby controls HSC homing to this area.[33] Up-regulation of TN-C expression within the central BM may functionally antagonize integrin α9 binding to osteopontin and enable it to promote HSC proliferation during hematopoietic recovery. Another known function for ECM molecules is the sequestration of growth factors and cytokines. We attempted to coimmunoprecipitate TN-C with the hematopoiesis-promoting cytokines SDF-1, SCF, and M-CSF, but failed to obtain positive results (data not shown). Therefore, the hematopoiesis-enhancing effect of TN-C seems to be restricted to its binding to integrin-expressing cells.

In conclusion, the results of the present study clarify the in vivo role of TN-C in supporting HSPC proliferation during BM reconstitution after myeloablation. Regulating the ECM should provide essential clues for the treatment of BM pathologies and for controlling normal hematopoiesis.

Acknowledgments

The authors thank Sakiko Kobayashi (Center for Integrated Medical Research, Keio University, Tokyo, Japan) for outstanding technical support.

This work was supported by Grants-in-Aid for Specially Promoted Research from the Ministry of Education, Culture,

Sports, Science and Technology of Japan; by a research grant from the Takeda Science Foundation; and by the Keio Kanrinmaru Project.

Authorship

Contribution: A.N.-I. performed the experiments, analyzed the data, and wrote the manuscript; Y. Okuno, Y. Omatsu, and K.O. performed the experiments and analyzed the data; J.M. and T.U. provided the TN-C^{FNIII} proteins and neutralizing Abs against integrin α9; T.N. analyzed the data and assisted in manuscript preparation; T.S. designed the experiments, interpreted the results, and assisted with manuscript preparation; and Y.K. designed the experiments, interpreted the results, and wrote the manuscript.

Conflict-of-interest disclosure: The authors declare no competing financial interests.

Correspondence: Toshio Suda, MD, PhD, or Yoshiaki Kubota, MD, PhD, Department of Cell Differentiation, The Sakaguchi Laboratory, School of Medicine, Keio University, 35 Shinanomachi, Shinjuku-ku, Tokyo 160-8582, Japan; e-mail: sudato@sc.itc.keio.ac.jp, or ykubo33@a3.keio.jp.

References

1. Schofield R. The relationship between the spleen colony-forming cell and the haemopoietic stem cell. *Blood Cells.* 1978;4(1-2):7-25.
2. Moore KA, Lemischka IR. Stem cells and their niches. *Science.* 2006;311(5769):1880-1885.
3. Wilson A, Trumpp A. Bone-marrow haematopoietic-stem-cell niches. *Nat Rev Immunol.* 2006; 6(2):93-106.
4. Taichman RS. Blood and bone: two tissues whose fates are intertwined to create the hematopoietic stem-cell niche. *Blood.* 2005;105(7):2631-2639.
5. Arai F, Hirao A, Ohmura M, et al. Tie2 / angiopoietin-1 signaling regulates hematopoietic stem cell quiescence in the bone marrow niche. *Cell.* 2004; 118(2):149-161.
6. Zhang J, Niu C, Ye L, et al. Identification of the haematopoietic stem cell niche and control of the niche size. *Nature.* 2003;425(6960):836-841.
7. Calvi LM, Adams GB, Weibrecht KW, et al. Osteoblastic cells regulate the haematopoietic stem cell niche. *Nature.* 2003;425(6960):841-846.
8. Kiel MJ, Yilmaz OH, Iwashita T, et al. Slam family receptors distinguish hematopoietic stem and progenitor cells and reveal endothelial niches for stem cells. *Cell.* 2005;121(7):1109-1121.
9. Kobayashi H, Butler JM, O'Donnell R, et al. Angiocrine factors from akt-activated endothelial cells balance self-renewal and differentiation of haematopoietic stem cells. *Nat Cell Biol.* 2010; 12(11):1046-1056.
10. Chow A, Lucas D, Hidalgo A, et al. Bone marrow CD169+ macrophages promote the retention of hematopoietic stem and progenitor cells in the mesenchymal stem cell niche. *J Exp Med.* 2011; 208(2):261-271.
11. Jaiswal S, Jamieson CH, Pang WW, et al. CD47 is upregulated on circulating hematopoietic stem cells and leukemia cells to avoid phagocytosis. *Cell.* 2009;138(2):271-285.
12. Sugiyama T, Kohara H, Noda M, Nagasawa T. Maintenance of the hematopoietic stem cell pool by CXCL12-CXCR4 chemokine signaling in bone marrow stromal cell niches. *Immunity.* 2006; 25(6):977-988.
13. Méndez-Ferrer S, Michurina TV, Ferraro F, et al. Mesenchymal and haematopoietic stem cells form a unique bone marrow niche. *Nature.* 2010; 466(7308):829-834.
14. Nilsson SK, Debatis ME, Dooner MS, et al. Immunofluorescence characterization of key extracellular matrix proteins in murine bone marrow in situ. *J Histochem Cytochem.* 1998;46(3):371-377.
15. Klein G, Beck S, Müller CA. Tenascin is a cytoadhesive extracellular matrix component of the human hematopoietic microenvironment. *J Cell Biol.* 1993;123(4):1027-1035.
16. Kubota Y, Takubo K, Suda T. Bone marrow long label-retaining cells reside in the sinusoidal hypoxic niche. *Biochem Biophys Res Commun.* 2008;366(2):335-339.
17. Zuckerman KS, Wicha MS. Extracellular matrix production by the adherent cells of long-term murine bone marrow cultures. *Blood.* 1983;61(3): 540-547.
18. Hsia HC, Schwarzbauer JE. Meet the tenascins: multifunctional and mysterious. *J Biol Chem.* 2005;280(29):26641-26644.
19. Gueders MM, Hirst SJ, Quesada-Calvo F, et al. Matrix metalloproteinase-19 deficiency promotes tenascin-C accumulation and allergen-induced airway inflammation. *Am J Respir Cell Mol Biol.* 2010;43(3):286-295.
20. Matsuda A, Yoshiki A, Tagawa Y, Matsuda H, Kusakabe M. Corneal wound healing in tenascin knockout mouse. *Invest Ophthal Vis Sci.* 1999; 40(6):1071-1080.
21. Koyama Y, Kusubata M, Yoshiki A, et al. Effect of tenascin-C deficiency on chemically induced dermatitis in the mouse. *J Invest Dermatol.* 1998; 111(6):930-935.
22. Soini Y, Kamel D, Apaja-Sarkkinen M, Virtanen I, Lehto VP. Tenascin immunoreactivity in normal and pathological bone marrow. *J Clin Pathol.* 1993;46(3):218-221.
23. Jones PL, Jones FS. Tenascin-C in development and disease: gene regulation and cell function. *Matrix Biol.* 2000;19(7):581-596.
24. Ohta M, Sakai T, Saga Y, Aizawa S, Saito M. Suppression of hematopoietic activity in tenascin-C-deficient mice. *Blood.* 1998;91(11):4074-4083.
25. Schreiber TD, Steinl C, Essl M, et al. The integrin alpha9beta1 on hematopoietic stem and progenitor cells: involvement in cell adhesion, proliferation and differentiation. *Haematologica.* 2009; 94(11):1493-1501.
26. Nakao N, Hiraiwa N, Yoshiki A, Ike F, Kusakabe M. Tenascin-C promotes healing of habu-snake venom-induced glomerulonephritis: studies in knockout congenic mice and in culture. *Am J Pathol.* 1998;152(5): 1237-1245.
27. Kanayama M, Kurotaki D, Morimoto J, et al. Alpha9 integrin and its ligands constitute critical joint microenvironments for development of autoimmune arthritis. *J Immunol.* 2009;182(12):8015-8025.
28. Kubota Y, Takubo K, Shimizu T, et al. M-CSF inhibition selectively targets pathological angiogenesis and lymphangiogenesis. *J Exp Med.* 2009; 206(5):1089-1102.
29. Morikawa S, Mabuchi Y, Kubota Y, et al. Prospective identification, isolation, and systemic transplantation of multipotent mesenchymal stem cells in murine bone marrow. *J Exp Med.* 2009; 206(11):2483-2496.
30. Omatsu Y, Sugiyama T, Kohara H, et al. The essential functions of adipo-osteogenic progenitors as the hematopoietic stem and progenitor cell niche. *Immunity.* 2010;33(3):387-399.
31. Yokosaki Y, Monis H, Chen J, Sheppard D. Differential effects of the integrins alpha9beta1, alphavbeta3, and alphavbeta6 on cell proliferative responses to tenascin. roles of the beta subunit extracellular and cytoplasmic domains. *J Biol Chem.* 1996;271(39):24144-24150.
32. Andrews MR, Czvitkovich S, Dassie E, et al. Alpha9 integrin promotes neurite outgrowth on tenascin-C and enhances sensory axon regeneration. *J Neurosci.* 2009;29(17):5546-5557.
33. Grassinger J, Haylock DN, Storan MJ, et al. Thrombin-cleaved osteopontin regulates hemopoietic stem and progenitor cell functions through interactions with alpha9beta1 and alpha4beta1 integrins. *Blood.* 2009;114(1):49-59.
34. Haylock DN, Nilsson SK. Osteopontin: a bridge between bone and blood. *Br J Haematol.* 2006; 134(5):467-474.
35. Adolfsson J, Borge OJ, Bryder D, et al. Upregulation of Flt3 expression within the bone marrow Lin(-)Sca1(+)c-kit(+) stem cell compartment is accompanied by loss of self-renewal capacity. *Immunity.* 2001;15(4):659-669.
36. Sato T, Laver JH, Ogawa M. Reversible expression of CD34 by murine hematopoietic stem cells. *Blood.* 1999;94(8):2548-2554.
37. Orend G, Huang W, Olayioye MA, Hynes NE, Chiquet-Ehrismann R. Tenascin-C blocks cell-cycle progression of anchorage-dependent fibroblasts on fibronectin through inhibition of syndecan-4. *Oncogene.* 2003;22(25):3917-3926.
38. Yokosaki Y, Matsuura N, Higashiyama S, et al. Identification of the ligand binding site for the integrin alpha 9beta 1 in the third fibronectin type III repeat of tenascin-C. *J Biol Chem.* 1998;273(19): 11423-11428.
39. Liao YF, Gotwals PJ, Koteliansky VE, Sheppard D, Van De Water L. The eiiia segment of fibronectin is a ligand for integrins alpha 9beta 1 and alpha 4beta 1 providing a novel mechanism for regulating cell adhesion by alternative splicing. *J Biol Chem.* 2002;277(17):14467-14474.
40. Yokosaki Y, Palmer EL, Prieto AL, et al. The integrin alpha 9 beta 1 mediates cell attachment to a non-RGD site in the third fibronectin type III repeat of tenascin. *J Biol Chem.* 1994;269(43): 26691-26696.
41. Wirl G, Hermann M, Ekblom P, Fässler R. Mammary epithelial cell differentiation in vitro is regulated by an interplay of EGF action and tenascin-C downregulation. *J Cell Sci.* 1995;108(Pt 6):2445-2456.
42. Yoshida T, Yoshimura E, Numata H, Sakakura Y, Sakakura T. Involvement of tenascin-C in proliferation and migration of laryngeal carcinoma cells. *Virchows Archiv.* 1999;435(5):496-500.